Vol. 35, No. 2 (2013) 141-147

Tribology in Industry

www.tribology.fink.rs

RESEARCH

Analyzing the Surface Roughness Effects on Piston Skirt EHL in Initial Engine Start-Up Using Different Viscosity Grade Oils

M. Gulzar[a], S.A. Qasim[a], R.A. Mufti[a]

[a] *College of Electrical and Mechanical Engineering, National University of Sciences and Technology (NUST), Pakistan.*

Keywords:

EHL
Piston skirt
Flow factor
Asperity
Hydrodynamic
Vogelpohl parameter

Corresponding author:

M. Gulzar
College of Electrical and Mechanical Engineering, National University of Sciences and Technology (NUST), Pakistan
E-mail: mubashir_nustian@hotmail.com

A B S T R A C T

The absence of fully developed fluid film lubrication between Piston and Liner surfaces is responsible for high friction and wear at initial engine start-up. In this paper flow factor method is used in two dimensional Reynolds' equation to model the effects of surface roughness characteristics on Piston Skirt elastohydrodynamic lubrication. The contact of surface asperities between the two surfaces and its after effects on EHL of piston skirt is investigated. For this purpose, two different grade oils are used to show the changing effects of viscosity combined with surface roughness on different parameters including film thickness, eccentricities and hydrodynamic pressures. The results of the presented model shows considerable effects on film thickness of rough piston skirt, hydrodynamic pressures and eccentricities profiles for 720 degrees crank angle.

1. INTRODUCTION

In initial engine start-up the piston and liner surfaces are not separated by an oil film which causes maximum wear and friction between the two sliding surfaces. The effects of physical contacts between the asperities of surfaces which are in relative motion must be included in lubrication model to get a better understanding of rheology. In lubricated interacting surfaces, the surface topography characteristics become more significant because they have a major effect on generation of a continuous lubricant film and in case of high amplitude of asperities in comparison to lubrication film thickness, there is an increased probability of direct contacts among asperities which can results in adhesive wear [1].

Hamilton, Wallowit and Allen [2] were the pioneer for taken into account the roughness effects on lubrication phenomenon and their work dates back to 1966. They developed a theory of hydrodynamic lubrication between two parallel surfaces with surface roughness on one or both of the surfaces. The classical theory of lubrication does not predict the existence of any pressure in case of sliding flat parallel surfaces. Surface roughness helps in the pressure build-up between the two interacting

surfaces, so provide a load support and avoid collapse of two bodies. Early research integrated the roughness amplitude with the film thickness and developed the modified one dimensional Reynolds's equation but the presented models did not cover different regimes and asperity contacts and limited to one dimensional changes. In this prospective an exception is given in 1978 and 1979 by Patir and Cheng [3-4]. Since the contacting surfaces have an inherent roughness, so Lambda Ratio or Tallian Parameter will be used as the defining parameter between different lubrication regimes [5]. In recent research the film thickness parameter (λ) range has been investigated and redefined for different lubrication regimes [6]. The P.C. model was suitable for values of film thickness ratio λ > 3 1.e; full film lubrication regime where asperity contacts were neglected [7-8]. To minimize the wear and friction losses the elastohydrodynamic lubrication (EHL) model is presented where λ is much lesser than a value of 3 [6]. Thus the flow factor model provided by J.H. Tripp [9] is numerically modelled for hydrodynamic lubrication at initial engine start-up. Greenwood-Tripp asperity contact model is used to incorporate the asperity contact forces and asperity contact friction force in EHL between the sliding surfaces [10]. To incorporate the isotropic behaviour the Peklenik number [11] is defined for the rough surfaces which are generated by normal distribution using Fast Fourier Transform [12-13]. In rheology a number of parameters affect the lubrication film between interacting surfaces. These parameters include piston to bore radial clearance, lubricant viscosities and chemical properties, surface roughness, shear heating, cavitation effects, squeeze film effects, material properties and other operating conditions.

The viscosities of lubricating oils along with characteristics of additives have a significant effect on friction and wear performance of interacting materials [14]. Thus in this research, isotropic rough piston and skirt surfaces are selected and modelled with high and low viscosity oils. The results are plotted, showing the hydrodynamic and EHL film thickness profiles, dimensionless eccentricities profiles and hydrodynamic pressures at 500 rpm with radial clearance of 10 micron. A comparison of the results for Oil A (0.016 Pa.s) and Oil B (0.1891 Pa.s) is provided. The results show an interesting finding, that the considered low viscosity oil (Oil A) is more suitable to avoid the contact and wear between interacting rough surfaces of piston and liner at initial engine start-up.

For developing the numerical model following assumptions are taken:

1. Lubricant is incompressible and thermal effects are neglected.
2. Non-Newtonian lubricant behaviour is neglected.
3. Pressure at the inlet is zero and surfaces are oil-flooded.
4. Lubricant flow is laminar and turbulence effects are neglected.
5. Leakage at the sides and edges is neglected.

2. NOMENCLATURE

C = Radial clearance between piston and liner = 10microns,

C_f = Specific heat of lubricant,

C_g = Distance from piston center of mass to piston pin = 0.2cm,

C_p = Distance of piston-pin from axis of piston = 1 cm,

F = Normal force acting on piston skirts,

F_f = Friction force acting on skirts surface,

F_{fh} = Friction force due to hydrodynamic lubricant film,

F_G = Combustion Gas force acting on the top of piston,

F_h =Normal force due to hydrodynamic pressure in film,

F_{IC} = Transverse Inertia force due to piston mass,

$\widetilde{F}_{IC}$ = Reciprocating Inertia force due to piston mass,

F_{IP} = Transverse Inertia force due to piston pin mass,

$\widetilde{F}_{IP}$ = Reciprocating Inertia force due to piston pin mass,

F_c = Asperity Contact Force,

F_{fc} = Friction force due to asperity contact,

G = Shear modulus of elastic lubricant,

I_{pis} = Piston inertia about its centre of mass,

M = Moment acting on piston skirts,

M_f = Friction moment acting on skirt surface,

M_{fh} = Moment about piston pin due to hydrodynamic friction,

M_h = Moment about piston pin due to hydrodynamic pressure,

M_c = Asperity Contact Moment,

M_{fc} = Moment due o friction force of asperity contact,

R = Radius of piston,

U = Piston Velocity,

a = Vertical distance from skirt top to piston-pin = 0.0125m,

b = Vertical distance from skirt top to piston center of gravity = 0.0015m,

e_t = Piston eccentricities at skirts top surface,

e_b = Piston eccentricities at skirts bottom surface,

$\ddot{e}_b$ = Acceleration of piston skirts bottom eccentricities,

$\ddot{e}_t$ = Acceleration of piston skirts top eccentricities,

h = Film Thickness,

l = Connecting rod length,

m_{pis} = Mass of piston = 0.295 kg,

m_{pin} = Mass of piston-pin = 0.09 kg,

p = Hydrodynamic pressure,

r = Crank radius = 0.0418 m,

ω = Constant crankshaft speed (engine speed),

τ = Shear stress,

η_A = Oil A viscosity = 0.016 Pa.s.,

η_B = Oil B viscosity = 0.1891 Pa.s.,

Φ = Connecting rod angle,

ψ = Crank angle,

ϕ_X, ϕ_y = Pressure flow factor along x and y-axis respectively,

ϕ_s = Shear flow factor,

σ = combined root mean square (rms) roughness,

σ_1 = rms roughness of piston skirt= 1.4μm,

σ_2 = rms roughness of cylinder liner = 1.5μm,

3. MATHEMATICAL MODEL

3.1 Equations of Piston Motion

The forces and moments are in the form of the force and moment balance equations similar to that defined by Zhu et al [15]:

$$\begin{bmatrix} a_{11} & a_{22} \\ a_{21} & a_{22} \end{bmatrix} \begin{bmatrix} \ddot{e}_t \\ \ddot{e}_b \end{bmatrix} = \begin{bmatrix} F_h + F_c + F_s + (F_{fh} + F_{fc}) \tan \Phi \\ M_h + M_c + M_s + M_f \end{bmatrix} \quad (1)$$

$$a_{11} = m_{pin}\left(1 - \frac{a}{L}\right) + m_{pin}\left(1 - \frac{b}{L}\right) \quad (2a)$$

$$a_{12} = m_{pin}\left(\frac{a}{L}\right) + m_{pin}\left(\frac{b}{L}\right) \quad (2b)$$

$$a_{21} = \left(\frac{I_{pin}}{L}\right) + m_{pin}(a-b)(1-\frac{b}{L}) \quad (2c)$$

$$a_{22} = m_{pin}(a-b)(\frac{b}{L}) - \left(\frac{I_{pin}}{L}\right) \quad (2d)$$

$$F_s = \tan \Phi \left(F_G + \tilde{F}_{IP} + \tilde{F}_{IC}\right) \quad (3)$$

$$M_s = F_G C_p + \tilde{F}_{IC} C_g \quad (4)$$

Using the Greenwood-Tripp's Asperity Contact Model, the values of F_c, F_{fc}, M_c and M_{fc} can be found for EHL regime [10].

3.2 Film Thickness Equation

The film thickness between the skirts and the liner given by Zhu [15]:

$$h = C + e_t(t)\cos x + \left[e_b(t) - e_t(t)\right]\frac{y}{L}\cos x \quad (6)$$

3.3 Reynolds' Equation Modelling

Modified 2-D Reynolds equation is given as [3]:

$$\frac{\partial}{\partial x}\left(h^3\phi_x\frac{\partial p}{\partial x}\right) + \left(\frac{R}{L}\right)^2\frac{\partial}{\partial y}\left(h^3\phi_y\frac{\partial p}{\partial y}\right) = 6U\eta\left(\frac{\partial h_T}{\partial x} + \sigma\frac{\partial \phi_s}{\partial x}\right) \quad (7)$$

where ϕ_x and ϕ_y are Poiseulle or pressure flow factors and ϕ_s is Cuotte or shear flow factor [3,9].

The boundary conditions are defined as [5]:

$$\frac{\partial p}{\partial x}_{\theta=0} = \frac{\partial p}{\partial x}_{\theta=\pi} = 0 \quad (8)$$

$p = 0$ when $x_1 \le x \le x_2$

$p(\theta,0) = p(\theta, L) = 0$

In dimensionless form the 2-D Reynolds equation is given by [5,9]:

$$\frac{\partial}{\partial x^*}\left(h^{*3}\phi_x\frac{\partial p^*}{\partial x^*}\right)+\left(\frac{R}{L}\right)^2\frac{\partial}{\partial y^*}\left(h^{*3}\phi_y\frac{\partial p^*}{\partial y^*}\right)=\frac{\partial h_T^*}{\partial x^*}+\sigma^*\frac{\partial \phi_S}{\partial x^*} \quad (9)$$

Where by J. H Tripp [9]:

$$\phi_X = 1+\left[3(\gamma-2)/(\gamma+1)\right][\sigma/h]^2\right]$$

$$\phi_y = \phi_X(1/\gamma)$$

$$\phi_s = \frac{\sigma_1^{\,2}}{\sigma^2}\phi_s(h/\sigma,\gamma_1) - \frac{\sigma_2^{\,2}}{\sigma^2}\phi_s(h/\sigma,\gamma_2)$$

$$\phi_s(h/\sigma,\gamma_2) = \left[\frac{3}{(\gamma+1)}(\sigma/h)\right]$$

and γ is the Peklenik number [11].

In order to read the pressure profiles conveniently, the Vogelpohl parameter M_v is introduced [5]:

$$M_v = p^* h^{*1.5}$$

The Reynolds equation in terms of the Vogelpohl parameter is given as:

$$\frac{\partial^2 M_v}{\partial .x^{*2}}+\left(\frac{R}{L}\right)^2\frac{\partial^2 M_v}{\partial .y^{*2}}+\left(\frac{\partial .\varphi_x}{\partial .x^*}(1/\varphi)\right)\left(\frac{\partial M_v}{\partial .x^*}\right)+ +\left(\frac{\partial .\varphi_y}{\partial .y^*}(1/\varphi)\right)\left(\frac{R}{L}\right)^2\left(\frac{\partial .M_v}{\partial .y^*}\right) = FM_v + G \quad (10)$$

where:

$$F = \frac{0.75\left[\left(\frac{\partial h^*}{\partial x^*}\right)^2+\left(\frac{R}{L}\right)^2\left(\frac{\partial h^*}{\partial y^*}\right)^2\right]}{h^{*2}} + \frac{1.5\left[\frac{\partial^2 h^*}{\partial x^{*2}}+\left(\frac{R}{L}\right)^2\frac{\partial^2 h^*}{\partial y^{*2}}\right]}{h^*} + \frac{1.5\left[\frac{\partial h^*}{\partial x^*}\left(\frac{\partial \varphi}{\partial x^*}\right)+\left(\frac{R}{L}\right)^2\frac{\partial \varphi}{\partial y^*}\left(\frac{\partial h^*}{\partial y^*}\right)\right]}{h^*\times\varphi}$$

$$G = \frac{\left(\frac{\partial h^*}{\partial x^*}+\sigma^*\frac{\partial \phi_S}{\partial x^*}\right)}{(h^{*1.5}\times\phi)}$$

$$M_{v,i,j} = \frac{C_{\cdot 1}\left(M_{v,i+1,j}+M_{v,i-l,j}\right)+\left(\frac{R}{L}\right)^2 C_{\cdot 2}\left(M_{v,i,j+l}+M_{v,i,j-l}\right)}{2.C_1+2.C_2+F_{i,j}} + \frac{C_{\cdot 3}\left(\frac{\partial .\varphi^*}{\partial .x^*}(1/\varphi^*)\right)\left(M_{v,i+1,j}-M_{v,i-l,j}\right)}{2.C_1+2.C_2+F_{i,j}} + \frac{C_{\cdot 4}\left(\frac{\partial .\varphi^*}{\partial .y^*}(1/\varphi^*)\right)\left(M_{v,i+1,j}-M_{v,i-l,j}\right)-G_{i.j}}{2.C_1+2.C_2+F_{i,j}}$$

3.4. Film Thickness in EHL Regime

In EHL regime the film thickness includes film thickness in the rigid hydrodynamic regime and the elastic surface displacements etc. By considering the bulk elastic deformation, the lubricant film thickness equation takes the following form [16]

$$h_{eh;} = h + f(\theta, y) + v$$

where $f(\theta, y)$ is neglected. The differential surface displacement is [16]:

$$dv = \frac{1}{\pi E'}\frac{p(x,y)\,dydy}{\dot{r}}$$

$$\dot{r} = \sqrt{(x-x_0)^2+\left[(y-y_0)^2\right]}$$

$$\frac{1}{E'} = \frac{1}{2}\left[\frac{(1-v_1^{\,2})}{E_1}+\frac{(1-v_2^{\,2})}{E_2}\right]$$

At a specific point (x_o, y_o) the elastic deformation is [5]:

$$v(x_0,y_0) = \frac{1}{\pi E'}\iint_a \frac{p(x,y)dxdy}{\dot{r}}$$

4. RESULTS AND DISCUSSION

The hydrodynamic lubrication and EHL models of the piston skirts at 500 rpm are developed after incorporating the pressure flow and the shear flow factors. Two different oils having viscosity 0.016 Pa.s and 0.1891 Pa.s are used for a comparison and investigating the viscosity effects on different parameters which include film thickness ,eccentricities and hydrodynamic pressure profiles at 720 degree crank rotation cycle.

4.1 Piston Eccentricities

The dimensionless eccentricities of the top and the bottom surface of the piston skirts (Et and

Eb) are plotted against the 720 degree crank rotation cycle. Figure 1(a) and 1(b) show eccentricity profiles for Oil A at 500 rpm. The results are plotted between a range of 1 and -1 where the physical contact between the sliding surfaces can occur. At central value '0' the motion is concentric. Figure 1(a) shows the dimensionless eccentricity profiles in the hydrodynamic lubrication regime whereas Fig. 1 (b) shows the similar profiles in the EHL regime.

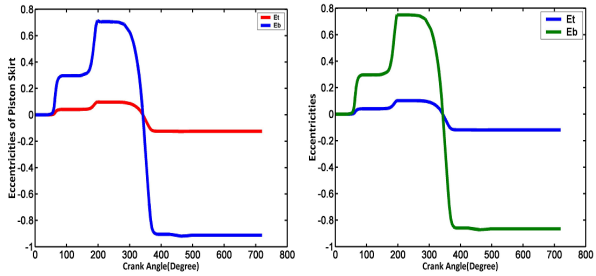

(a) (b)

Fig. 1. For Oil A, Dimensionless Eccentricities at 500 rpm in (a) Hydrodynamic regime (b) EHL Regime.

The behaviour is shown for all the four strokes where it can be seen that at the start of cycle the piston and liner axis are concentric then due to the secondary motion the profiles are highly displaced from the centre towards thrust side and non-thrust side, but for Oil A the physical contact is avoided as shown in Fig. 1. For Oil B, the dimensionless eccentricities profiles for hydrodynamic and EHL regime are shown in Fig. 4. Figure 4 (a) shows that the contact is established at lower surface as line is meeting with -1 in rigid hydrodynamic regime. However in Fig. 4 (b) the EHL regime shows the physical contact is clearly avoided. This shows that the elastic deformation of asperities help in avoiding the contact between interacting surfaces, thus help in avoiding friction related wear.

Comparison of eccentricities for both oils provides an interesting finding that the low viscosity oil can be more helpful at initial engine start-up speed of 500 rpm for rigid hydrodynamic regime as well as equally good for EHL regime.

4.2 Hydrodynamic Pressures

Three dimensional pressure fields and related pressure distribution are plotted for 720 degree crank angle. Figures 2 (a), 2(b), 2(c), 2(d) show 3-D hydrodynamic pressure profiles at 900, 4500, 6300 and 7200 crank angles at 500 rpm. The positive pressures are developed over the piston skirt and vary as shown in Fig. 2. In Fig. 2 (a), for Oil A, at 90 degrees crank angle the pressures are biased towards bottom of piston skirt and extended to the middle of piston skirt. The peak pressure occurs at the bottom of piston skirt. In Fig. 2 (b), for Oil A, at 450 degrees crank angle, the pressure field shows that the hydrodynamic pressures are developed at top of piston skirt though a small ridge can be seen at bottom of piston Skirt. The peak pressures are larger than the 90 degrees angle. In Fig. 2 (c), at 630 degrees crank angle, the pressures are shifted towards top of piston skirt. In Fig. 2(d), at 720 degrees the pressure profile is more steep and developed at bottom of piston skirt showing the end of cycle. For Oil B, in Fig. 5(a), 5(b), 5(c), 5(d) show 3- D hydrodynamic pressure profiles at 900, 4500, 6300 and 7200 crank angles at 500 rpm speed.

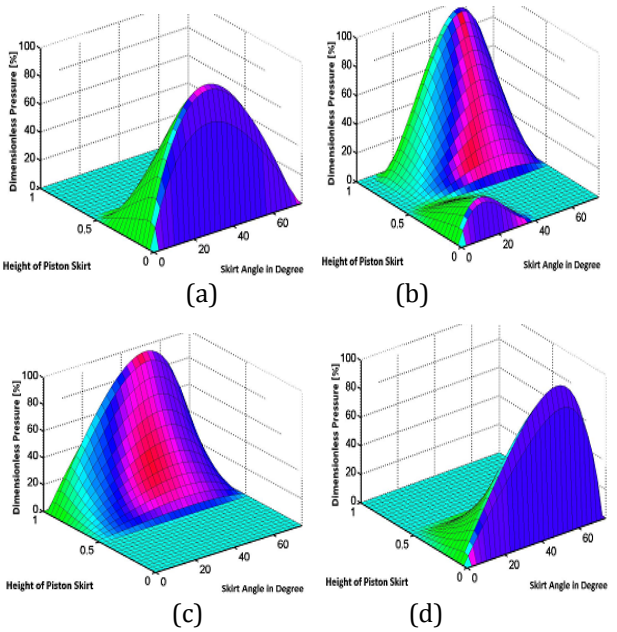

(a) (b)

(c) (d)

Fig. 2. For Oil A, 3-D Hydrodynamic pressure fields at 500 rpm at crank angle (a) 90 degree (b) 450 degree (c) 630 degree (d) 720 degree.

For the pressure fields it can be clearly investigated that the hydrodynamic pressures are totally shifted towards top of piston skirt at 450 degrees crank angle while the case was not same in case of Oil A for similar conditions. The major change in shape of pressure filed can be observed for 630 degrees crank angle where the dimensionless pressure is biased towards bottom of piston skirt instead of top as discussed for Oil A. Thus changing the viscosity of oil is affecting the distribution of hydrodynamic pressures over piston skirt.

4.3 Hydrodynamic and EHL Film Thickness

Figure 3(a) shows the maximum and the minimum hydrodynamic film thickness for Oil A at 500 rpm and 10 micron radial clearance. The maximum film thickness is calculated before the application of load and on the other side the minimum film thickness is found after the application of load. The magnitude of minimum film thickness shows whether the film thickness is capable of avoiding the contact between sliding surfaces or not. In Fig. 3(a), the minimum hydrodynamic film start getting established from start of cycle and reaches at a peak at power stroke and decrease to minimum at end of exhaust stroke and cycle continues. Similar case can be seen for Oil B in Fig. 6(a), but the difference is evident at end of exhaust stroke where a second peak of film thickness can be seen. In Fig. 3(b) and 6(b) EHL film thickness profiles are shown. By comparing both profiles, it can be seen that in case of Oil A the EHL film thickness is greater in magnitude for different crank angles as compare to Oil B. Thus Oil A, which is low viscosity oil, will be more helpful in avoiding the contact and wear between rough piston and liner surfaces.

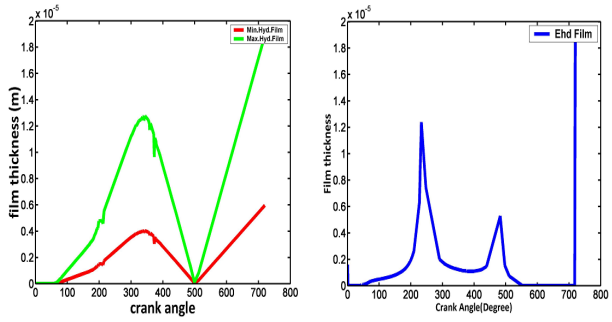

(a) (b)

Fig. 3. For Oil A, At 500 rpm (a) Film thickness profiles (b) EHL film.

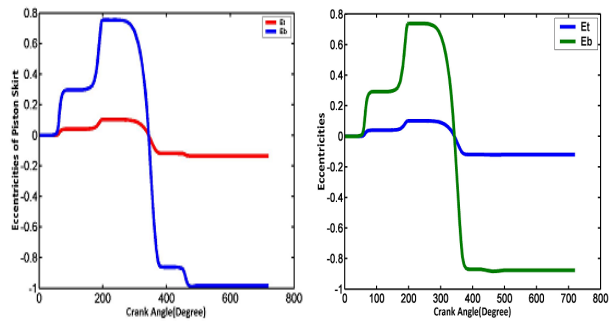

(a) (b)

Fig. 4. For Oil B, Dimensionless Eccentricities at 500 rpm in (a) Hydrodynamic regime (b) EHL Regime.

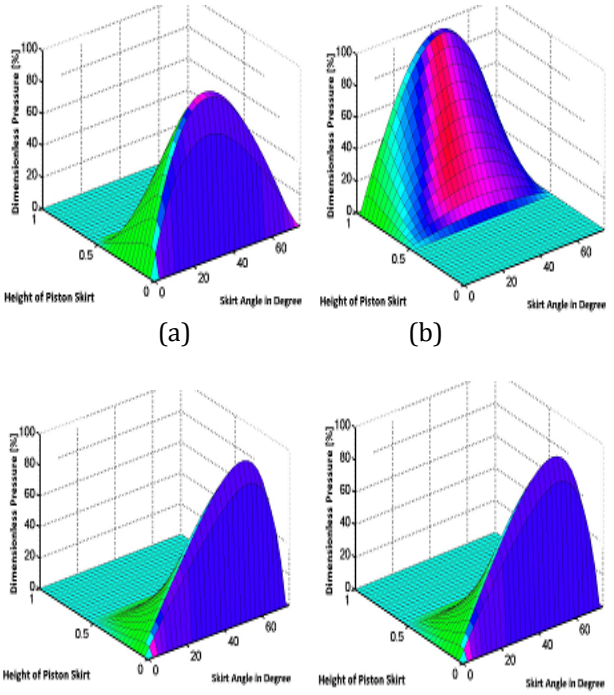

(a) (b) (c) (d)

Fig. 5. For Oil B, 3-D Hydrodynamic pressure fields at 500 rpm at crank angle (a) 90 degree (b) 450 degree (c) 630 degree (d) 720 degree.

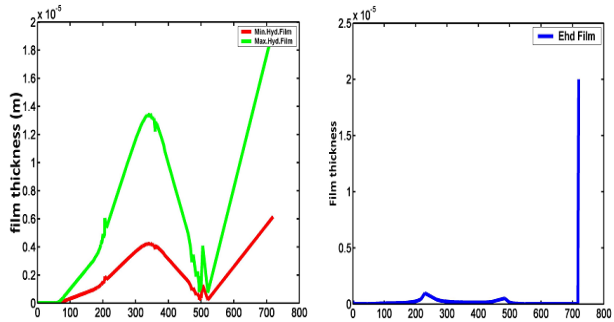

(a) (b)

Fig. 6. For Oil B, At 500 rpm (a) Film thickness profiles (b) EHL film.

5. CONCLUSION

Two dimensional numerical models for hydrodynamic and EHL regimes were developed at initial engine start-up speed for isotropic rough piston skirt and cylinder. Two different grade oils were used to investigate the different parameters affecting the rough piston skirt wear phenomenon. The different rough surfaces of the interacting skirts and the liner were considered by introducing the pressure and the shear flow factors in the lubrication model. For Oil 'B' having a viscosity of 0.1891 Pa.s, the simulation results verify that a physical contact between

the rough skirts and the liner surfaces cannot be avoided in the rigid hydrodynamic regime. However, for both oils, the rough interacting surfaces deform elastically to generate a sufficiently thick film in the EHL regime. The hydrodynamic pressures shifting occur from top of piston skirt to bottom at 630 degrees crank angle by changing Oil A to Oil B at 500 rpm and 10 micron radial clearance. Comparing both oils for given conditions, Oil A is more suitable to avoid the contact and wear between interacting rough surfaces.

REFERENCES

[1] N. Diaconu, L. Deleanu, F. Potecasu, S. Ciortan: *The Influence of the Relative Sliding on the Surface Quality,* Tribology In Industry, Vol. 33, No. 3, pp. 110-115, 2011.

[2] D.B. Hamilton, J.A. Walowit, C.M. Allen: *Theory of Lubrication by Microirregularities*, Journal of Basic Engineering, Trans ASME, Vol. 88, No. 1, pp. 177-185, 1966.

[3] N. Patir, H.S. Cheng: *An Average Flow Model for Determining Effects of Three-Dimensional Roughness on Partial Hydrodynamic Lubrication*, ASME Journal of Lubrication Technology, Vol. 100, No. 1, pp 12-17, 1978.

[4] N. Patir, H.S. Cheng: *Application of Average Flow Model to Lubrication Between Rough Sliding Surfaces*, ASME Journal of Lubrication Technology, Vol. 101, No. 2, pp. 220-230, 1979.

[5] G.W. Stachowiak, A.W. Batchelor: *Engineering tribology*, 3rd ed., Elsevier, pp. 328, 2005.

[6] Dong Zhu, Q Jane Wang: *On the λ ratio range of mixed lubrication*, Proc IMechE Part J: Journal of Engineering Tribology, Vol. 226, No. 12, pp. 1010–1022, 2012.

[7] J.H. Tripp, B.J. Hamrock: *Surface roughness effects in elastohydrodynamic contacts*, in: Proc 1984 Leeds Lyon Symposium on Tribology 1985, pp. 30–9.

[8] H.G. Elrod, A. General: *Theory for Laminar Lubrication with Reynolds Roughness*, ASME Journal of Lubrication Technology, Vol. 101, No. 1, pp. 8-14, 1979.

[9] J.H. Tripp: *Surface Roughness Effects in Hydrodynamic Lubrication: The Flow Factor Method*, ASME Journal of Lubrication Technology, Vol. 105, pp 458-463, 1983.

[10] J.A. Greenwood, J.H. Tripp: *The Contact of Two Nominally Flat Rough Surface*, Proc. Institution of Mechanical Engineers (IMechE), UK, (185), pp 625-633, 1971.

[11] J. Peklenik: *New Developments in Surface Characterization and Measurement by Means of Random Process Analysis*, Proc. Instn. Mech. Engrs., Vol. 182, pp. 108-125, 1967-68.

[12] N. Garcia, E. Stoll: *Monte Carlo Calculation of Electromagnetic-Wave Scattering from Random Rough Surfaces*, Physical Review Letters, Vol. 52, No. 20, pp. 1798-1801, 1984.

[13] FFTW library - free collection of fast C routines for computing discrete Fast Fourier Transforms. Developed at MIT by Matteo Frigo and Steven G. Johnson.

[14] A. Vadiraj, G. Manivasagam, K. Kamani, V.S. Sreenivasan: *Effect of Nano Oil Additive Proportions on Friction and Wear Performance of Automotive Materials,* Tribology In Industry, Vol. 34, No. 1, pp. 3-10, 2012.

[15] D. Zhu, Y. Hu, H.S. Cheng, T. Arai, K. Hamai: *A numerical Analysis for Piston Skirts in Mixed Lubrication, Part 2: Deformation Consideration*, ASME Journal of Tribology, Vol. 115, No. 1, pp. 125-133, 1993.

[16] S.A. Qasim, M.A. Malik, M.A. Khan, R.A. Mufti: *Low Viscosity Shear Heating in Piston Skirts EHL in the Low Initial Engine Start Up Speeds*, Tribology International, Vol. *44,* No. 10, pp. 1134-1143, 2011.